Seismic analysis of overhead crane bridges using friction-based sliding model

J. . Colomb[1], D. Bouhjiti[1], N. Anishchenko[1], Y. Shaparevich[1], E. Bou Said[1]

[1] Egis, Montreuil, France (david.bouhjiti@egis.fr)

INTRODUCTION

Crane bridges are handling devices used to lift and transfer heavy loads, widely used in the industry, including the nuclear industry. Assessing the dynamic behavior of crane bridges may constitute an important issue for nuclear safety: within the context of seismic Level 1 Probabilistic Safety Assessment (PSA) studies, these devices have been identified as significant contributors in the probability of core meltdown. Moreover, modelling the mechanical behavior of such a device under seismic load is a challenging scientific and engineering exercise, due to the importance of contact dissipative phenomena such as friction, sliding and impacts in determining their dynamic response.

The behavior of the anchoring seems to be the primary cause of failure of this equipment when loading is supposed beyond design conditions. Consequently, it is necessary to enhance the knowledge on the mechanical behavior of this equipment in order to fully understand its response to earthquakes and, in particular, to assess the efforts transmitted to the anchorages.

To that aim, (SOCRAT benchmark, 2021) consists of a large experimental program on a 1:5 scaled model of an overhead crane bridge submitted to various loading configurations on the shaking table of French Sustainable Energies and Atomic Energy Commission (CEA). The obtained results are used to characterize and calibrate the FE models to assess their predictive capacities in case of high intensity earthquakes.
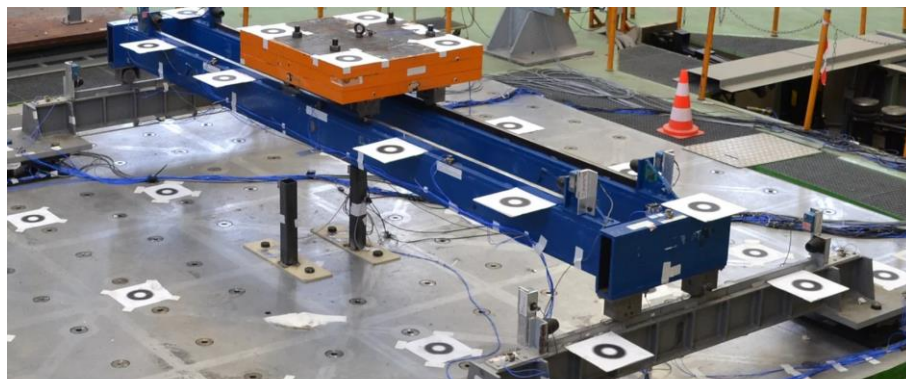

Figure 1. Illustration of the 1:5 scaled overhead crane bridge (SOCRAT) on the shaking table

In this paper, EGIS shares its modelling strategy, results and feedback related to the specific issue of overhead crane bridge modelling with a focus on the definition of friction coefficients (of wheels) and the effect of their variation on the obtained structural response

FINITE ELEMENTS MODEL

The model is established using ANSYS Mechanical APDL software (implicit solver) and the crane bridge is modelled using a full shell-based approach (8 nodes per shell element with 6 degrees of freedom per each node: 3 displacements and 3 rotations). The reference 3D CAD of the SOCRAT mock-up, the elastic material properties and the seismic loadings was provided by the benchmark organizers (SOCRAT benchmark, 2021).

Geometry and Mesh generation

The crane bridge is decomposed into several structural parts as detailed in the following figure and table:
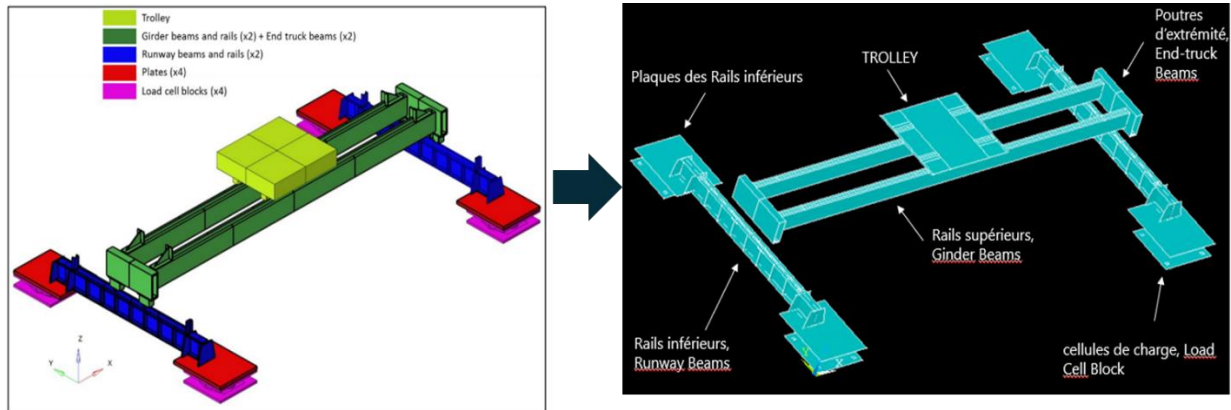

Figure 2. Shell based geometry editing from the 3D CAD data

Table 1: Structural parts of the crane bridge

Structural part	FE type	Mass (tons)	Dimensions
Runway beams	Shell281	1.19	Length: 2.6 m – Height: 24 cm Width: 10.6 cm – Flange thickness: 13 mm Web thickness: 9 mm
Runway rails	(not modelled)	-	
Girder beams	Shell281	1.37	Length: 5.0 m – Height: 25 cm Width: 11 cm – thickness: 30 mm
Girder rails	(not modelled)	-	
End truck beams	Shell281	0.19	
Wheels supports	Rigid	0.00	
Load cells' plates	Shell281	0.25	Section: 65 cm x 65 cm – height: 17 cm Thickness: 30 mm
Load cells	Matrix27	-	
Trolley	Shel281	1.60	Length: 110 cm – Width: 10.2 cm Height: 21 cm
Total	9912 finite elements	4.60	

The rails upon which the wheels can slide or roll, the wheels' supports and the wheels themselves are not explicitly represented in the model. For the sake of simplification, only equivalent contact areas are modelled ensuring two contact zones for each wheel: (a) lateral contact between the wheel and the lateral edge of the rail and (b) horizontal contact between the wheel and the upper surface of the rail. The wheel supports are considered rigid to ensure the effort transfer from the wheel to the beams.
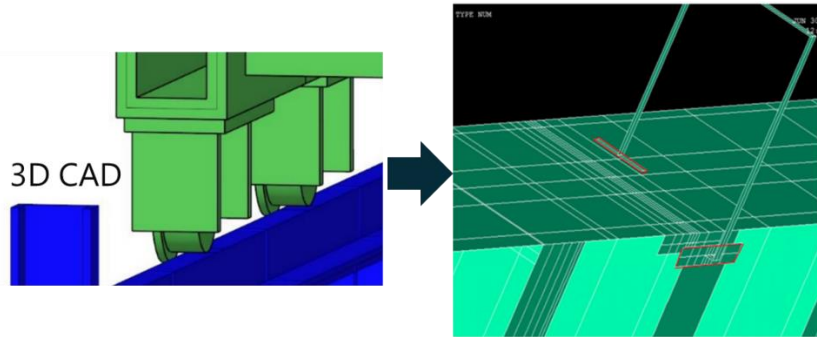

Figure 3. Equivalent modelling of the wheel-rail contact (surface to surface)

Finally, the load cells at the bottom of the bridge are modelled using springs with three translation and three rotational stiffness values.

Material properties

The used properties for each structural part are presented hereafter:

Table 2: Structural parts of the crane bridge

Structural part	Mass density (kg/m3)	Young's modulus (GPa)	Poisson's ratio (-)	Yield stress (MPa)
Runway beams	7800	210	0.3	355
Girder beams	8000	210	0.3	355
End truck beams	8000	210	0.3	355
Wheels supports	7800	210	0.3	355
Wheels	7700	200	0.3	350
Load cells' plates	7800	210	0.3	355
Trolley	7800	210	0.3	-
	Horizontal stiffness	Vertical stiffness	Rotational stiffness	Torsional stiffness
Load cells	614 MN/m	2710 MN/m	7.41 MNm/rad	4.86 MNm/rad

Behaviour law

All steel elements are considered linear elastic within the framework of the present study. The only non linearity that is considered is due to the contact modelling between the wheels and the rails.

In total, there are 4 wheels between the trolley and the girder beam and 4 wheels between the girder and runaway beams. The main sliding directions of each group are perpendicular to each other: the trolley can move along the girder beam length whilst the trolley+girder can move along the runway beam length.

The standard Coulomb's law of friction is used within a pair based contact and an isotropic friction coefficient. The damping is activated according to the Rayleigh method with a structural damping of 4%. The additional viscous damping is provided by the nonlinear contact modelling is activated. One should note that no dissipation associated to eventual shocks is accounted for.

In the absence of prior experimental data, a constant isotropic steel to steel friction coefficient of 0.3 is considered. Eventually, if needed, this value is updated along the various studied configurations.

Loading combinations

Several loading configurations are investigated experimentally within this benchmark:
- Centred vs. decentred trolley positions
- Sliding vs. rolling wheels
- Impulsive signal vs. 2D seismic load vs. 3D seismic load
- Low amplitude vs. high amplitude signals (0.5g to 1.5g) applied at the bottom of the cell load plates (bolted to the shaking table).

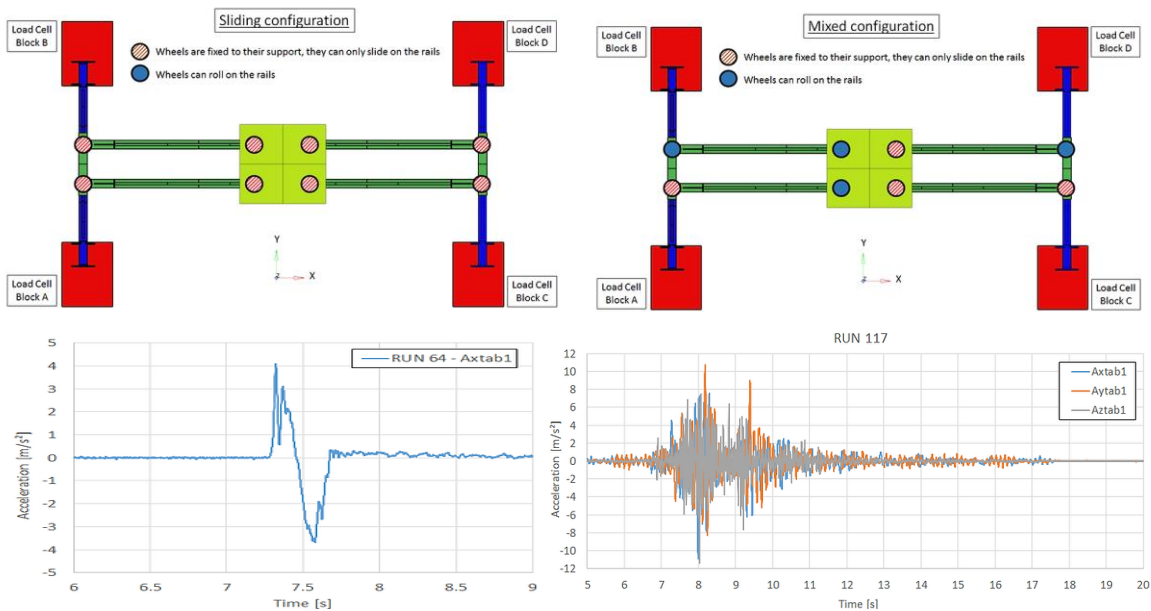Examples of such loads (in terms of acceleration) are presented hereafter:

Figure 4. Examples of studied configurations within the SOCRAT benchmark

Details for all loadings and configurations are provided in (SOCRAT benchmark, 2021).
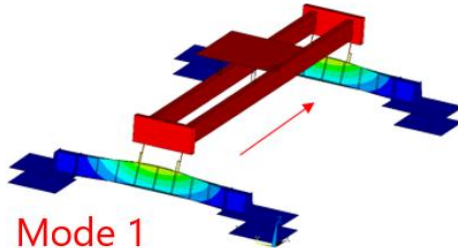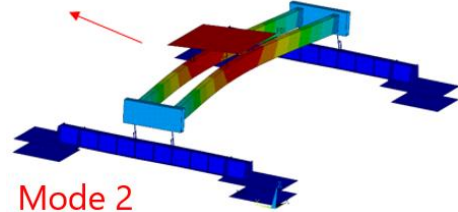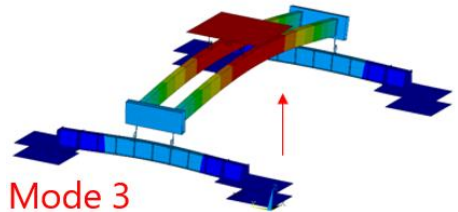
MODEL VALIDATION

For model validation, calculations are limited to static and modal analyses.

Under dead load, one gets a numerical deflection around 1.7mm of the trolley (centred position) which is very close to the measured displacement.

As for the modal analysis of the whole mock-up, one gets the following results:

Table 3: Eigenfrequencies analysis (numerical vs. experimental)

Experimental frequency (Hz)	Numerical frequency (Hz)	Numerical effective mass (%)	Modal deformation
7.6	8.2	66	Mode 1
8.3	8.4	56	Mode 2
13.2	12.8	59	Mode 3

To achieve modal analysis, contact surfaces are supposed closed and bonded (no sliding). The lower plates of the load cells are fixed. The obtained blind results a maximal relative error of 7% for the mode 1 and are, therefore, considered satisfactory.

FITTING STRATEGY

The response (in terms of displacements) of the crane bridge seems very sensitive to various parameters: initial position of the wheel on the rail (the maximal gap between the wheel and the lateral edge of the rail is of 14 mm), the surface state (damage, stripes or defects), the evolution of the friction as the loading increases or decreases (dependence on the velocity), etc. In the present benchmark, all these elements are not known a priori and make difficult blind calculations of the bridge's behaviour (as it is the case for full scale and operational bridges). To simplify the inverse problem as much as possible, only one parameter is considered for updating: the friction coefficient of each wheel group.

Therefore, one should keep in mind that such updating accounts for other uncertainties and not only the one of the friction coefficient. The idea is to define a range of values that one can uses for blind calculations without enriching the model further (to keep the computational time reasonable – around few hours at most).

RESULTS PREVIEW

Transient analysis N°1

In this case study, the trolley is considered centred, all the wheels can slide and the loading is applied along the x direction. The displacement measurements are achieved at points A, B, C and D (see picture below).
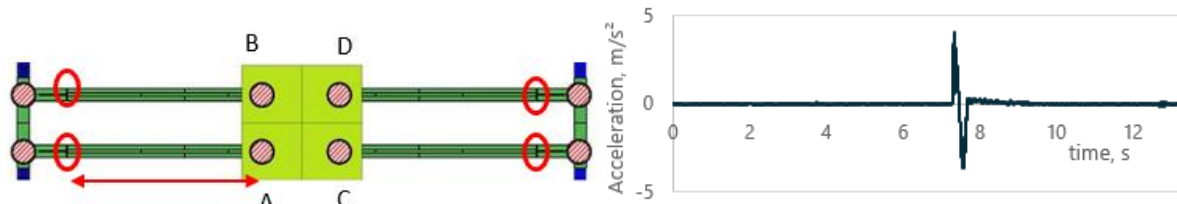
Figure 5. Case study N°1: centred – sliding – impulse 0.5g – direction x

The blind calculations (with a default friction coefficient of 0.3) show an underestimated residual displacement of the trolley (2mm compared to 8mm measured experimentally). By inverse analysis, and using a friction coefficient for the upper wheels of 0.242, one reaches the 8mm amplitude.
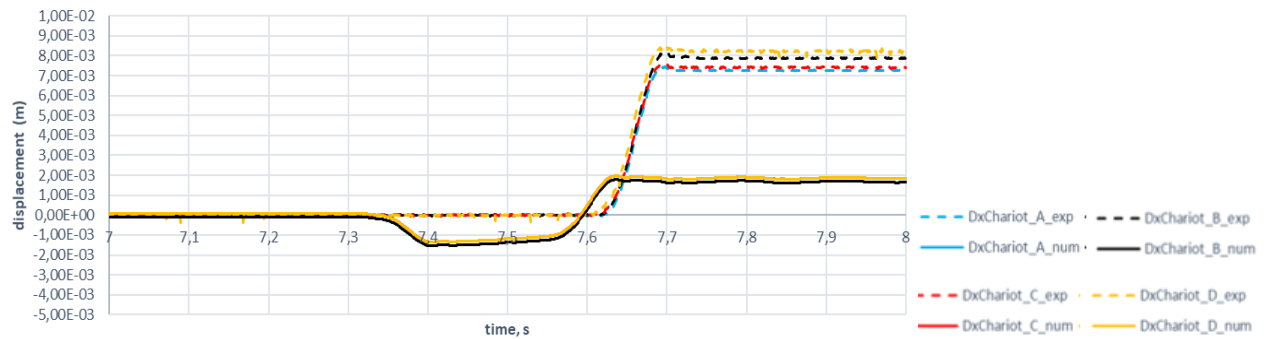

Figure 6. Case study N°1: Numerical vs. experimental displacements (prior estimation)
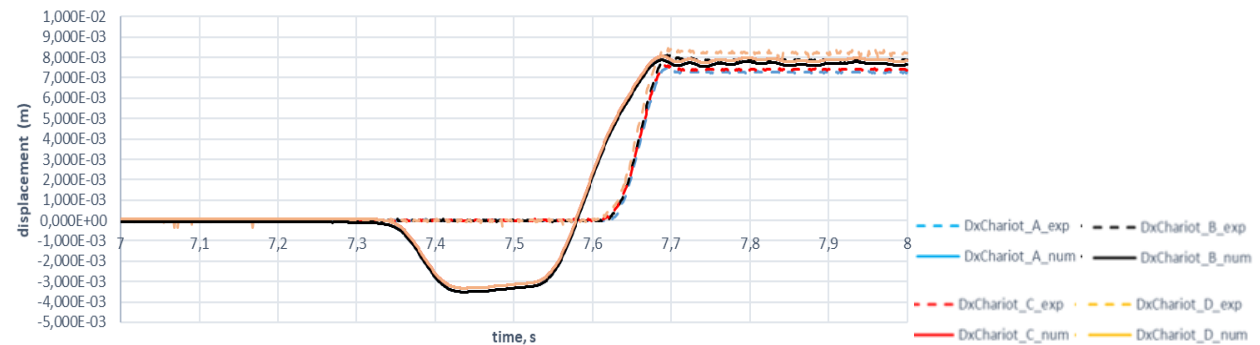

Figure 7. Case study N°1: Numerical vs. experimental displacements (posterior estimation)

Given the nature of the loading, the displacement along the y direction remains negligible.

Transient analysis N°2

In this case study, the trolley is considered centred, all the wheels can slide and the loading is applied along the y direction. The displacement measurements are achieved at points A, B, C and D (see picture below).
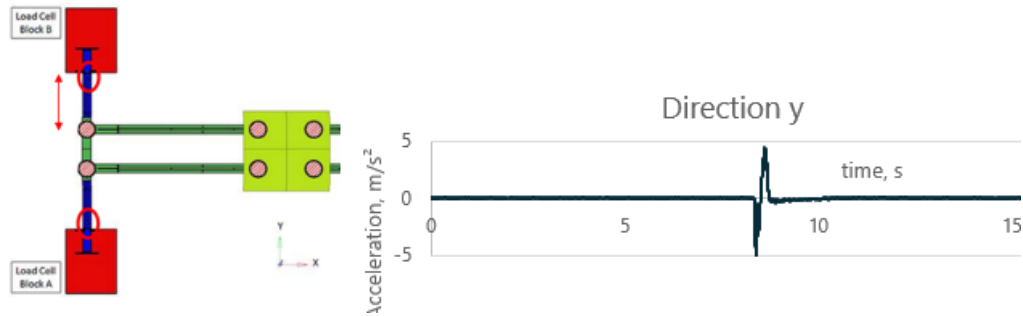

Figure 8. Case study N°2: centred – sliding – impulse 0.5g – direction y

The blind calculations (with a default friction coefficient of 0.3) show an underestimated residual displacement of the girder beams (1cm vs. 3cm measured experimentally) and do not allow the representation of asymmetric behavior (up to 2cm gap between the two sides of the trolley measured experimentally). By inverse analysis, and using two different friction coefficients for each side of the runway beams (0.294 on one side and 0.291 on the other), one manages to represent accurately the observed behaviour.
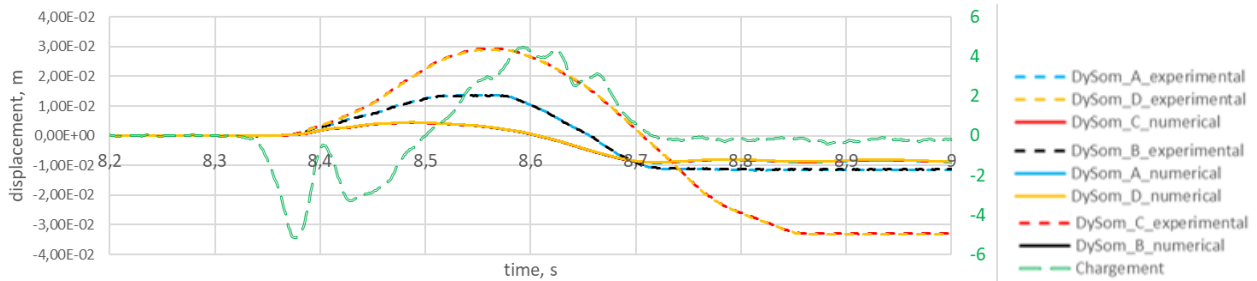

Figure 9. Case study N°2: Numerical vs. experimental displacements (prior estimation)
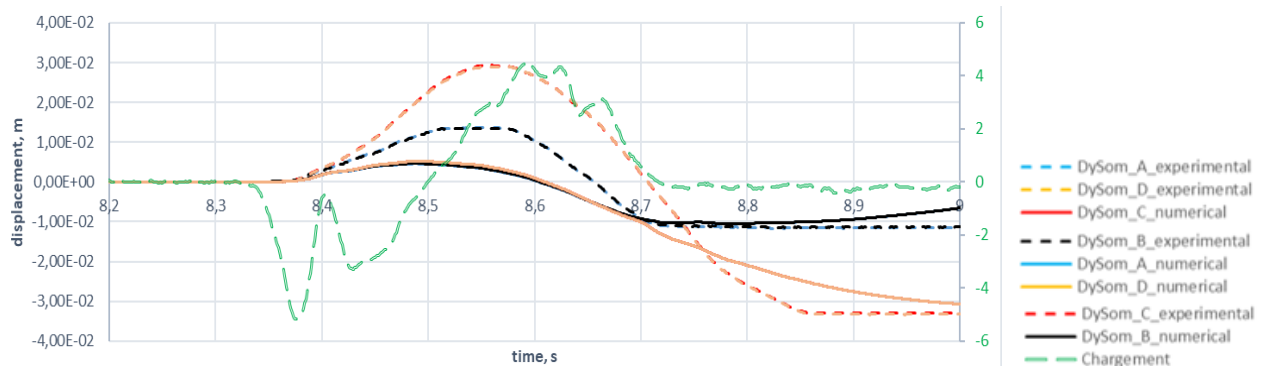

Figure 10. Case study N°2: Numerical vs. experimental displacements (posterior estimation)

Given the nature of the loading, the displacement along the x direction remains negligible.

Transient analysis N°2bis

This case study is similar to the previous one (N°2) with imposed loading in the y direction, a reduced acceleration (0.2g) with a mixed slide-roll configuration (two wheels under the girder can slide and two others can roll).
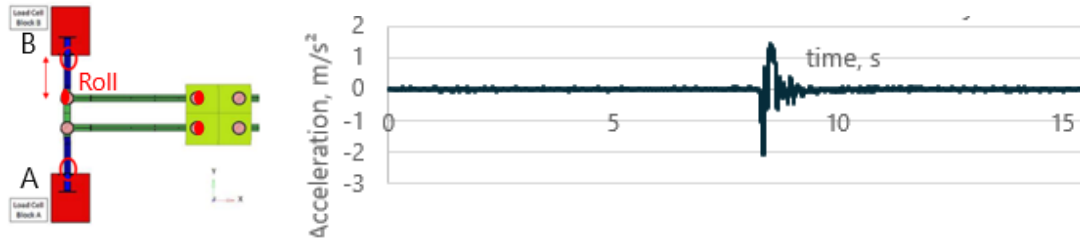

Figure 11. Case study N°2bis: centred – sliding/rolling – impulse 0.2g – direction y

To obtain similar results to the ones observed experimentally, the use of smaller friction coefficients (than 0.3) is needed. By inverse analysis, one gets 0.13 on one side and 0.15 on the other side (these coefficients are defined only for sliding wheels under the girder beam).
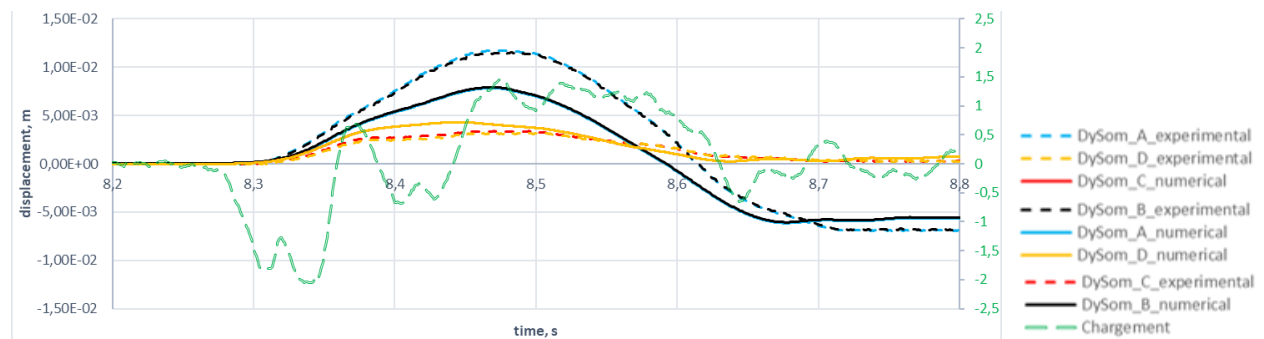

Figure 12. Case study N°2bis: Numerical vs. experimental displacements (posterior estimation)

Transient analysis N°3

In this case study, the trolley is considered decentred, all the wheels can slide and the loading is applied along the x, y and z directions. The displacement measurements are achieved at the trolley and girder beam level (see picture below).
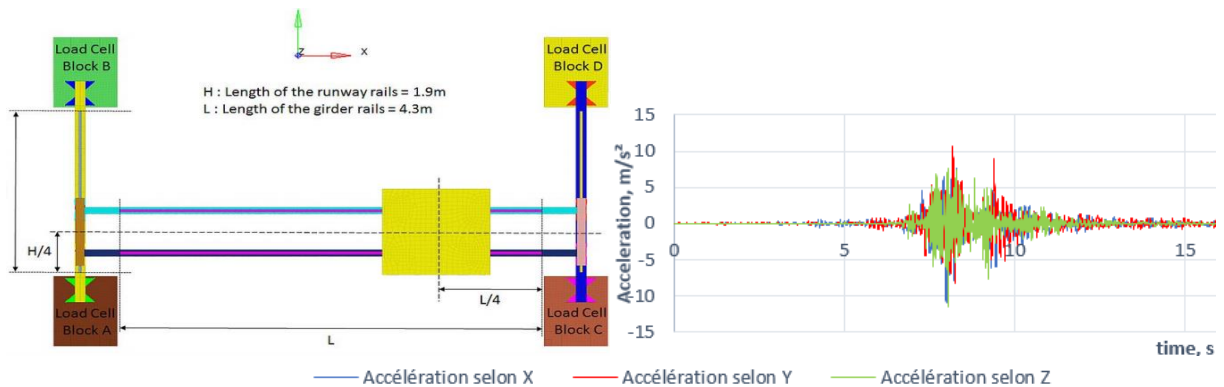

Figure 13. Case study N°3: decentred – sliding – seismic load 1g – direction x,y,z

The applied loading leads to 3d displacements of the structural parts; the trolley along the x/z directions and the girder beam along the y/z directions. To get the same displacements as the ones measured experimentally (best fit for the residual displacement), the inverse analysis leads to a friction coefficient of 0.28 for the wheels under the trolley and 0.1 for wheels under the girder beam.
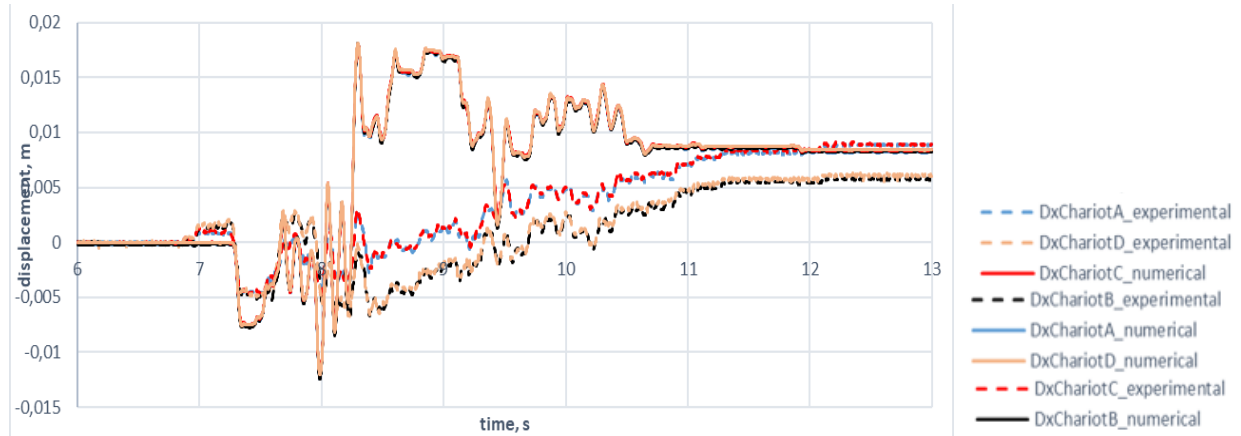

Figure 14. Case study N°3: Numerical vs. experimental displacements of the trolley along the x direction (posterior estimation)
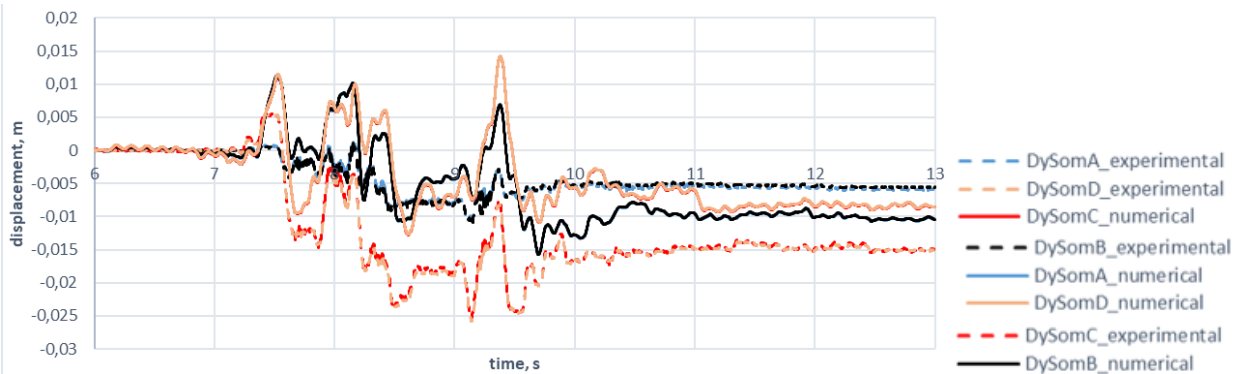

Figure 15. Case study N°3: Numerical vs. experimental displacements of the girder beam along the y direction (posterior estimation)
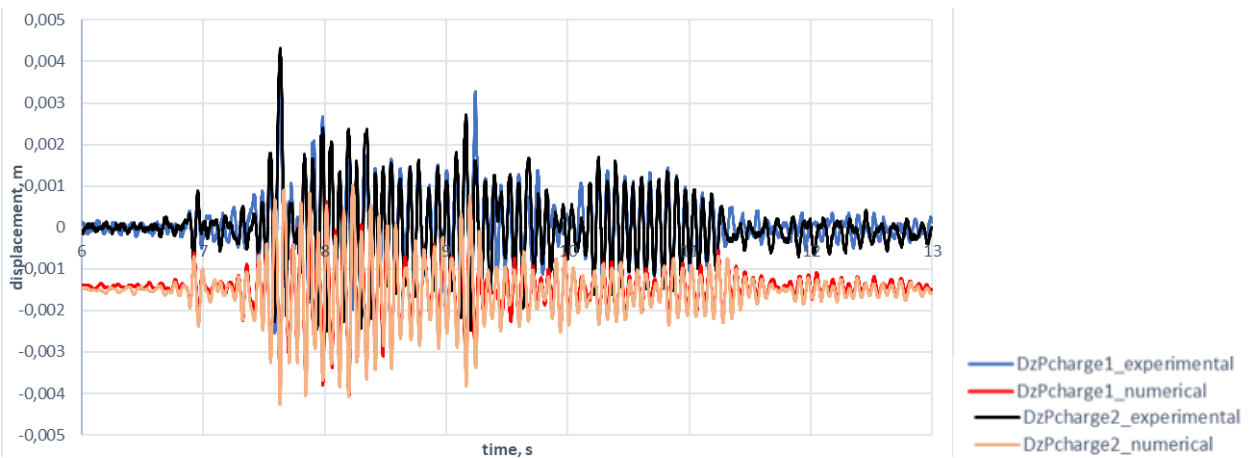

Figure 16. Case study N°3: Numerical vs. experimental displacements of the girder beam along the z direction (posterior estimation)

The calibration for such realistic seismic loading is hard to achieve for all the time steps and all directions. So, the quantity of interest is limited to the residual displacement of each structural part. In the vertical direction, calculations are in line with measured values (regardless of the applied friction coefficients).

CONCLUSION

The modelling of the SOCRAT crane bridge mock-up demonstrates the high sensitivity of the bridge's response to the friction coefficients of its wheels. This makes any blind calculation hard to achieve and encourages the consideration of advanced sensitivity analyses or probabilistic approaches to cope with the several uncertainties related to the crane bridges behaviour (effect of friction anisotropy, effect of dynamic loading on the friction properties, geometrical defects, damping issues, etc.).

Within the analysed case studies, we observe that the range of values for the friction coefficients varies between 0.01 (rolling condition) to 0.28 (sliding condition) for the various wheels. Higher values seem to be applicable to the upper wheels whilst the lower wheels show lower friction coefficients under seismic loads.

Ideally, to forecast an envelope behaviour of the crane bridge one can run several nonlinear analyses using various combinations of the friction coefficients. However, given the computational time that this might lead to, the model needs to be kept simplified (accounting for most important phenomena) and the numerical design plan efficiently defined using adapted sampling techniques coupled to the expert judgement (one might have from available feedbacks on the issue of interest).

REFERENCES

SOCRAT benchmark website: *https://www.socrat-benchmark.org/,* 2021